Materials Science & Engineering C 102 (2019) 756–763

Contents lists available at ScienceDirect

Materials Science & Engineering C

journal homepage: www.elsevier.com/locate/msec

Chondrogenesis of human mesenchymal stem cells by microRNA loaded triple polysaccharide nanoparticle system

Ekin Çelik[a], Cem Bayram[b], Emir Baki Denkbaş[c,d,*]

[a] Kırşehir Ahi Evran University, Faculty of Medicine, Medical Biology Department, 40100 Kırşehir, Turkey
[b] Hacettepe University, Advanced Technologies Application and Research Center, 06800, Beytepe, Ankara, Turkey
[c] Başkent University, Faculty Engineering, Biomedical Engineering Department, 06530, Bağlıca, Ankara, Turkey
[d] Hacettepe University, Graduate School of Science and Engineering, Bioengineering Division, 06800, Beytepe, Ankara, Turkey

ARTICLE INFO

Keywords:
Hyaluronic acid
Chitosan
Chondroitin sulfate
Micro RNA
Nanoparticle
Chondrogenesis

ABSTRACT

Degenerative cartilage is the pathology of severe depletion of extracellular matrix components in articular cartilage. In diseases like osteoarthritis, misregulation of microRNAs contributes the pathology and collectively leads to disruption of the homeostasis. In this study chondroitin sulfate/hyaluronic acid/chitosan nanoparticles were prepared and successfully characterized chemically and morphologically. Results demonstrated higher chondroitin sulfate amounts led smaller nanoparticles, but lower surface zeta potential due to high electronegativity. After optimization of chondroitin sulfate amounts regarding size and charge, nanoparticles were loaded with microRNA-149-5p, a therapeutic miRNA downregulated in osteoarthritis, and evaluated focusing on their loading efficiency, release behaviour, cytotoxicity and gene transfection efficiency in vitro. Results showed all nanoparticle formulations were non-toxic and promising gene delivery agents, due to increased levels of microRNA-149-5p and decreased mRNA levels of microRNA's target, FUT-1. Highest gene transfection efficiency was obtained with the nanoparticle formulation which had the highest chondroitin sulfate load and smallest size. In addition, owing to their high chondroitin sulfate cargo, all nanoparticles were reported to enhance chondrogenesis, which was demonstrated by gene expression analysis and sulfated glycosaminoglycan (sGAG) staining. The obtained data suggest that the delivery of microRNA-149-5p via polysaccharide based carriers could achieve collaborative impact in cartilage regeneration and have a potential to enhance osteoarthritis treatment.

1. Introduction

Articular cartilage is a well specialized tissue found in knee joints. It provides lubrication, articulation and load distribution, assisting knee movements [1]. Articular cartilage can be damaged due to trauma, environmental factors, age, genetics or systemic diseases and its healing abilities are restricted due to lack of blood and lymphatic vessels, which limits its recovery so challenges patients and doctors [2]. Many therapies used in clinic involve invasive procedures such as microfracture, drilling, abrasion arthroplasty, autologous chondrocyte implantation, osteochondral autograft transplantation and osteochondral allograft transplantation [3]. Apart from these surgical procedures, viscosupplement injections have emerged as non-operative tools to manage degenerative cartilage symptoms, serving as only pain relievers, without affecting the course of the disease [4].

Articular cartilage have a dense extracellular matrix, which contains mainly collagens and proteoglycans with a synovial tissue providing viscosity and lubricity owing to its high hyaluronic acid (HA) content [2]. The primary function of HA is to preserve synovial fluid viscosity, along with facilitating proteoglycan synthesis, controlling inflammatory responses and maintaining the cartilage matrix [5,6]. In osteoarthritis, cartilage degenerates and synovial fluid viscosity, so water content decreases together with hyaluronic acid volume. Thus, intra-articular viscosupplementations with HA injections emerged in an attempt to recover the normal viscoelastic character of knee to promote HA synthesis and delay its degradation [4,7–9].

In articular cartilage, proteoglycans, mainly chondroitin sulfate, provide elasticity to tissue, also promoting collagens to fulfil their role for providing tensile strength [10]. In degenerative cartilage case, however, both chondroitin sulfate and hyaluronic acid content are known to be deceased, which in turn cause articular cartilage to loose its elasticity, viscosity and water content, and mechanical durability obliquely as well, due to extracellular matrix disruption [11].

Regarding all these molecular changes occurring in the

* Corresponding author at: Başkent University, Faculty Engineering, Biomedical Engineering Department, 06530, Bağlıca, Ankara, Turkey.
E-mail address: denkbas@hacettepe.edu.tr (E.B. Denkbaş).

https://doi.org/10.1016/j.msec.2019.05.006
Received 4 February 2019; Received in revised form 29 April 2019; Accepted 3 May 2019
Available online 03 May 2019
0928-4931/

degenerating cartilage, scientists have been studying on reconstitution of these macromolecules to restore its viscoelastic properties, along with delivery of therapeutical agents to enhance tissue healing [12–15]. Lately, a variety of carriers like nanoparticles, hydrogels, scaffolds and nanogels have been developed to reduce degeneration and shown a great potency to enhance tissue healing and integrity [16–20]. Pi et al. showed that siRNA encapsulated PEI-peptide nanoparticles (NPs) have successfully lessen cartilage degeneration in mice [21]. Jeon et al. used siRNA and SOX-9 releasing PLGA NPs to induce chondrogenesis in human mesenchymal stem cells [22]. Ding-Lu and colleagues proved hyaluronic acid-chitosan particles as plasmid carriers for targeting osteoarthritis in 2011 [23]. When it comes to polysaccharides, hydrogel networks stand out as delivery systems owing to their water adsorption capacity [24]. Bian et al. showed alginate microspheres inside a hyaluronic acid hydrogel manage to enhance chondrogenesis in mesenchymal stem cells [25]. Kim and colleagues used oxidized hyaluronate and glycol chitosan hydrogels to encapsulate chondrocytes, Qi et al. formed injectable sericin hydrogels to repair cartilage [26,27]. Lately, nanogel systems emerged for more effective drug/gene delivery, which are described as distributions of hydrogel nanoparticles from polymeric networks and advantageous regarding low-toxicity and ease of handling [28]. Nochi and colleagues formed nanogels for adjuvant free intranasal vaccination and Li et al., recently reported a bioreduction-ruptured polymer nanogel system for siRNA delivery [29,30].

MicroRNAs (miRNAs) are naturally occurring small, single-stranded noncoding RNAs which are post-transcriptionally controlling gene expression [31,32]. They appear to be key players in regulation of several biochemical pathways and homeostasis and deregulation of miRNAs has been shown to cause diseases including osteoarthritis. miRNAs in cartilage play important roles in chondrogenesis, cartilage development and homeostasis [33]. In degenerating cartilage, mainly the expression of miRNAs which play role in extracellular matrix (ECM) production is known to decrease [34]. Restoration of these miRNAs with synthetic mimics has been showed to promote endogenous miRNAs to re-gain their functions and enhance the expression of ECM matrix components [12,35,36].

MicroRNA-149-5p is a 23-mer small RNA, which has shown to mediate chondrocyte proliferation, apoptosis and autophagy in cartilage, especially during osteoarthritis. Overexpression of microRNA-149-5p is reported to induce proliferation and prevent apoptosis of chondrocytes, thus prevent osteoarthritis [37]. It is also showed to be downregulated in osteoarthritis patients, causing degenerated cartilage and damaging homeostasis [31].

Herein this study, we investigated the effect of overexpression of microRNA-149-5p on mesenchymal stem cells in vitro, carried with chondroitin sulfate coated hyaluronic acid-chitosan nanoparticles. Particle size and surface zeta potential, morphology, particle stability and degradation, microRNA encapsulation efficiency and in vitro release profiles were determined. Cytotoxicity and transfection efficiency of nanoparticles were further investigated in vitro.

2. Materials and methods

2.1. Materials

Chitosan (CS) with a molecular weight of 150 kDa and a deacetylation degree of 80% was purchased from Sigma (St. Louis, USA). TPP was obtained from Sigma (St. Louis, USA). HA was obtained from Acros Organics (USA) with a molecular weight of 1,5mDa. Chondroitin sulfate (ChoS) was bought from Sigma (St. Louis, USA). The miRNA 149-5p sequence (5′-UCUGGCUCCGUGUCUUCACUCCC-3′) used in this study was purchased from Qiagen (Germany).

2.2. Preparation of ChoS (HA/CS) NPs and miRNA-149-5p loaded ChoS (HA/CS) NPs

0.6125 mg/mL (3.8 μM) chitosan and 1.25 mg/mL (0.83 μM) hyaluronic acid was dissolved in nuclease-free water. Blank HA/CS NPs were synthesized by slowly adding of HA solution to chitosan solution in different mass ratios by the ionotropic gelation methods [38]. The nanoparticle solutions were prepared with HA:CS ratios of 1:1, 1:2, 1:4, 1:6, 1:10. Briefly, 50 μL of TPP (cross-linker) solution were first mixed with 0.83 M HA solution and the resulting HA-TPP solution was added dropwise to different volumes of chitosan solution [39]. Solutions were mixed on magnetic stirrer for 20 min, then incubated for 20 min at room temperature to stabilize nanoparticles. The nanoparticles were then centrifuged at 3500*g* for 5 min, and supernatants were collected.

Blank ChoS (HA/CS) NPs were prepared by addition of varying concentrations of chondroitin sulfate solution onto 1:4 HA/CS NPs via ionic interaction [40]. 2.29 μM, 3.44 μM, 4.59 μM, 5.73 μM, 6.88 μM, 8.03 μM, 9.17 μM, 10.32 μM, 11.47 μM and 13.76 μM ChoS (HA/CS) NPs were prepared.

MicroRNA attached ChoS (HA/CS) NPs were formed via ionic interactions. After synthesis and stabilization of ChoS (HA/CS) NPs, microRNA solutions were added onto nanoparticle solutions dropwise with 30:1 N:P ratio.

2.3. Physiochemical characterization of nanoparticles and their encapsulation efficiencies

Physiochemical properties of nanoparticles were assessed by dynamic light scattering (DLS) with ZetaSizer Nano series Nano-ZSP (Malvern Instruments, Malvern, UK). Each sample was studied in triplicate.

Morphological examination of nanoparticles was performed with scanning electron microscopy (SEM), after washing nanoparticles three times prior to visualisation.

To determine encapsulation efficiencies of nanoparticles and free microRNA were recovered from the supernatant via centrifugation at 13,000 rpm for 10 min. The encapsulation efficiency of nanoparticles were calculated with the following formula: Encapsulation efficiency (%) = (A − B)/A × 100. A is the total weight of added microRNA and B is the weight which is recovered from supernatant after centrifugation at high speed. The amount of free microRNA was measured with Qubit 3.0 fluorometer (Thermo Fischer Scientific, US) using microRNA assay kit.

2.4. The stability of nanoparticles and the controlled release of microRNA 149-5p from nanoparticles in vitro

Nanoparticles without microRNA loads were suspended in deionized water, PBS and 10% serum containing DMEM under mild stirring at 37 °C. The sizes were determined at day 0, 1, 2 and 3 via dynamic light scattering (DLS) technique to determine degradation profiles of nanoparticles.

To examine release behaviour of microRNA-149-5p from nanoparticles, nanoparticles were suspended in nuclease free water and put on dialysis within dialysis membranes with molecular weight cut off 20,000 Da at 37 °C in a water bath. The released microRNA was monitored at indicated time intervals over 7 days by Qubit fluorometer after centrifugation.

2.5. Gel retardation assay

MicroRNA interaction on nanoparticles was analyzed by 2% gel electrophoresis. The gels were prepared with 2% agarose gel in 1 × TBE buffer with ethidium bromide to a final concentration of 0.2 μg/mL. Gel electrophoresis was carried out at 80 V for 10 min and the gel was subsequently photographed in gel imaging system (ChemiDoc-It

Imager, UVP). Nanoparticles were degraded with SDS for 20 mins prior to loading, to prove nanoparticle interaction.

2.6. Cytotoxicity assays

Cytotoxicity of nanoparticles was evaluated via 3-(4,5-dimethylthiazol-2-yl)-2,5-diphenyltetrazolium bromide (MTT) assay (Glentham Life Sciences). Chondrocytes at a density of 5×10^4 cells/mL were seeded into 96-well plates 24 h prior to experiment. The cells were then incubated with nanoparticles for 24 h. Subsequently, 13 μL of MTT solution (5 mg/mL in phosphate-buffered saline (PBS), PanBiotech) and 100 μL of fresh media were added. After 4 h of incubation at 37 °C, medium in each well was replaced with 100 μL of isopropanol solution (containing 0.04 N HCl) to dissolve the formazan crystals. The plate was incubated once again for 20 min in dark and absorbance was measured at 570 nm using a microplate reader (SpectroStar Nano, BMG Labtech). Each sample group was studied in 8 replicates with 500 μg/mL, 250 μg/mL, 125 μg/mL and 62.5 μg/mL concentrations.

2.7. MicroRNA transfection

Human mesenchymal stem cells were cultured in %10 FBS containing DMEM (Life Sciences, BI) media supplemented with 10% FBS (Gibco-BRL) and incubated at 37 °C in a humidified atmosphere with %5 CO_2. For transfection experiments, cells were seeded in a 6-well plate (2×10^6 cells per well) and incubated with nanoparticles with a 100 nM microRNA concentration, in 1 mL serum-free DMEM media for 6 h. Subsequently, cell culture with 10% FBS added onto cells and cultured for 48 h. Afterwards cells were harvested for gene expression analysis.

2.8. Gene expression analysis

RNA isolation was performed according to manufacturer's protocol (PureLink RNA mini kit, Thermo Fisher Scientific), DNAse I treatment was performed during isolation to obtain high yield. Isolated RNAs were then reverse transcribed with High Capacity Reverse Transcription Kit (Applied Biosystems, Thermo Fisher Scientific) on ice, due to kit protocol with random primers except miRNA-149-5p at conditions 25 °C for 10 min, 37 °C for 120 min and 85 °C for 5 min. Stem-loop primer used for reverse transcription of miRNA-149-5p was as follows; 5′-GTTGGCTCTGGTGCAGGGTCCGAGGTATTCG- CACCAG AGCCAACGGGAGT-3′. GAPDH was used as internal control. The primers used in the experiment are ACTB: F primer, CATGTACGTTGCTA TCCAGGC, R primer, CTCCTTAATGTCACGCACGAT, FUT-1: F primer, CCTGGCATCTTCTGGAGAAGCT, R primer, TTCTAGAACTGCCTGCCA GCCAT, miRNA-149-5p: F primer, GTTTCTGGCTCCGTGTCTT, R primer, GTGCAGGGTCCGAGGT, SOX-9: F primer, GTACCCGCACTTG CACAAC, R primer, TCTCGCTCTCGTTCAGAAGTC, COMP: F primer, AACTCAGGGCAGGAGGATGT, R primer, TGTCCTTTTGGTCGTCGTTC, COL2A1: F primer, AAAAGAGGTGCCCGTGGAGAA, R primer, TTGCC TTGAGGACCAGCATCA, AGC: F primer, GGGGACCTTAGTGGACTTCC TTCTG, R primer, AGGTCCACCCCAGAATACTCACC. Gene expression studies were performed with comparative CT method using Viia7 Real-Time PCR System (Thermo Fisher Scientific) with PowerUp SYBR Green Master Mix (Thermo Fisher Scientific). Each sample was performed in three replicates.

2.9. Sulfated glycosaminoglycan (sGAG) staining

Mesenchymal stem cells were incubated with nanoparticles for 56 h and stained with Safranin O Staining Kit (ScienCell) according to manufacturer's instructions. Cells were washed with sterile PBS prior to staining.

2.10. Statistical analysis

The mean ± SD was determined for each experiment group. Statistical differences between groups were evaluated with one way ANOVA test, by using the GraphPad Prism software version 6 (GraphPad Software, La Jolla, USA). P value was considered as 0.05. Level of significance was represented as follows: $p > 0.05$ as not significant, $p \leq 0.05$ as *, $p \leq 0.01$ as **, $p \leq 0.001$ as ***, and $p \leq 0.0001$ as ****.

3. Results and discussion

3.1. Characterization of ChoS (HA/CS) NPs

Dynamic light scattering analysis was performed to assess the physiochemical properties of ChoS (HA/CS) NPs and microRNA 149-5p incorporated ChoS (HA/CS) NPs. Prior to chondroitin sulfate interaction, HA/CS nanoparticles were synthesized with different mass:mass ratios, 1:1, 1:2, 1:4, 1:6, 1:10 (Supplementary Table 1). As the nanoparticles were designed to be gene carriers, chitosan amounts were increased to maintain high positive charge. Nanoparticles with highest surface charge and smallest size were obtained in 1:4 HA:CS (m:m) formulation, so following experiments were conducted with 1:4 HA/CS nanoparticles.

The effect of chondroitin sulfate incorporation on the average hydrodynamic diameter and surface zeta potential of nanoparticles is shown in Table 1. HA:CS NPs with 1:4 (m:m) ratio were interacted with different amounts of chondroitin sulfate as following: 2.29 μM, 3.44 μM, 4.59 μM, 5.73 μM, 6.88 μM, 8.03 μM, 9.17 μM, 10.32 μM, 11.47 μM, 13.76 μM.

It is observed that surface charge of the nanoparticles decreased with increasing chondroitin sulfate concentration, because of large anionic groups of chondroitin sulfate. It also affected nanoparticle size, forming strong electrostatic interactions with protonated amines of chitosan, hence caused nanoparticles to shrink in size [41]. After 10.32 μM chondroitin sulfate inclusion, nanoparticles began to increase in size, as excess negatively charged components of chondroitin sulfate led to repulsive forces upon competition for positively charged amines of chitosan [42,43]. Following experiments were performed with 4.59 μM, 6.88 μM and 9.17 μM ChoS (HA/CS) NPs, and denoted as NP1, NP2 and NP3, respectively.

Although the infrared spectra of chondroitin sulfate, hyaluronic acid and chitosan show quite overlapping peaks due to their polysaccharide structure, there were some changes showing the structural differentiation (Fig. 1). The multiple peaks observed between 1050 and 1200 cm^{-1} after chondroitin sulfate addition indicate presence of sulfate groups. In addition, N—H stresses observed in the presence of chitosan contributed to the large O—H peak of chondroitin sulfate and were observed as two overlapping peaks after addition to the nanoparticles. The spectra at 1350–1400 cm^{-1} confirm the presence of strong sulfate peaks as well.

Table 1
DLS measurements of chondroitin sulfate incorporated HA/CS NPs.

ChoS load	Charge	Size	PDI
2.29 μM	27.40 mV ± 0.77	450.8 nm ± 10.1	0.63
3.44 μM	27.02 mV ± 1.29	403.9 nm ± 10.6	0.51
4.59 μM	26.33 mV ± 2.02	383.6 nm ± 11.5	0.42
5.73 μM	25.01 mV ± 1.26	375.0 nm ± 13.8	0.40
6.88 μM	24.13 mV ± 1.58	357.8 nm ± 12.0	0.33
8.03 μM	16.75 mV ± 2.14	315.4 nm ± 11.2	0.29
9.17 μM	11.40 mV ± 1.41	320.2 nm ± 11.3	0.20
10.32 μM	7.04 mV ± 1.68	362.6 nm ± 18.9	0.34
11.47 μM	5,68 mV ± 2.50	425.1 nm ± 20.1	0.56
13.76 μM	−1.55 mV ± 4.09	467.7 nm ± 32.9	0.80

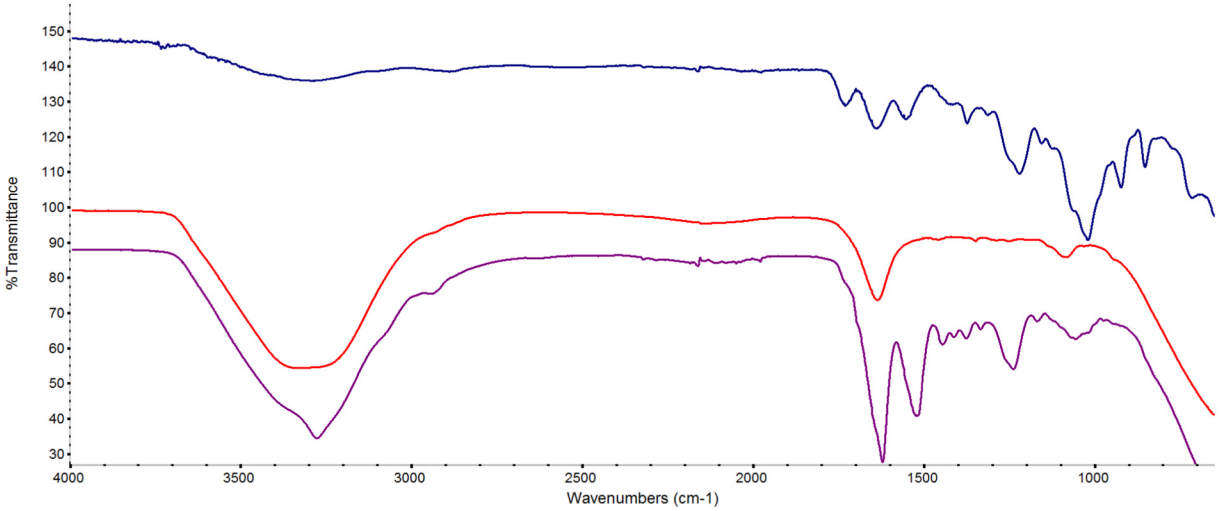

Fig. 1. FT-IR spectra of nanoparticles. Blue spectra shows chondroitin sulfate, red spectra shows HA/CS NPs, purple spectra shows chondroitin sulfate coated HA/CS (NP2) nanoparticles. (For interpretation of the references to color in this figure legend, the reader is referred to the web version of this article.)

Table 2
Size and charge measurements and loading efficiencies of ChoS (HA/CS) NPs.

	Charge	Size	+RNA (charge)	+RNA (size)	Loading efficiency
NP1	26.33 mV ± 2.02	383.6 nm ± 11.5	17.51 mV ± 2.15	412.26 nm ± 21.18 (PDI 0.4)	84.13%
NP2	24.13 mV ± 1.58	357.8 nm ± 12.0	15.76 mV ± 1.59	259.45 nm ± 13.89 (PDI 0.24)	73.87%
NP3	11.40 mV ± 1.41	320.2 nm ± 11.3	9.23 mV ± 1.38	180.20 nm ± 10.23 (PDI 0.19)	60.97%

MicroRNAs were attached to the surface of nanoparticles and the size and surface charge of NP1, NP2 and NP3 nanoparticles and loading efficiencies after microRNA interaction are given in Table 2.

Various types of nanomaterials have been used as gene delivery agents. Wang et al. used nanostructured lipid nanoparticles for micro RNA transfection, in which they achieved a nearly 70% loading efficiency [44]. Zhang et al. reported 80% micro RNA loading efficiency for their nanoparticles [45]. Herein, we obtained 84.13%, 73.87% and 60.97% gene loading efficiency for NP1, NP2 and NP3, respectively.

The morphology of ChoS (HA/CS) NPs was observed using SEM (Fig. 2). Nanoparticles were shown to retain their spherical shape. Although particles were washed via dialysis prior to SEM imaging, nanoparticles seem to be aggregated after drying and coating process due to excess polymer in the solution.

SEM images correlates with the DLS measurements, revealing the decrease in size of ChoS (HA/CS) nanoparticles with increasing chondroitin sulfate amounts. In addition, higher chondroitin sulfate content led lessened aggregation of HA/CS NPs, due to stabilized forces among anionic and cationic groups (Fig. 3).

3.2. Stability of ChoS (HA/CS) NPs

Stability of nanoparticles was tested in 3 different media, prior to microRNA loading. ChoS (HA/CS) NPs were studied in nuclease-free water, PBS and DMEM medium supplemented with %10 FBS. Stability experiments were performed at 37 °C for 72 h and the size of nanoparticles were measured in every 24 h (Fig. 3). The results showed nanoparticles maintained their size without degradation after 72 h. No aggregation was observed. NP2 nanoparticles were studied for stability experiments of ChoS (HA/CS) NPs. ChoS (HA/CS) NPs were shown to increase their size more than HA/CS NPs, due to the higher amount of polysaccharides. Nanoparticles increase their size 42.66% in nuclease

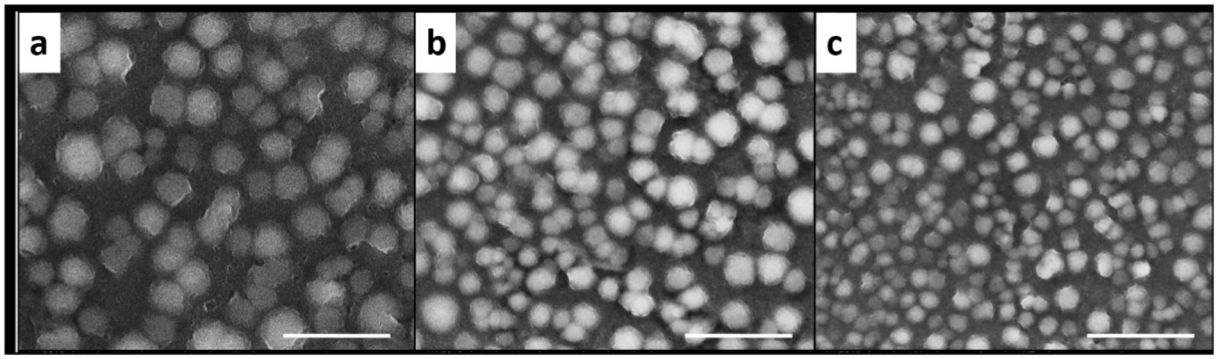

Fig. 2. SEM images of nanoparticles interacted with chondroitin sulfate (a) NP1, (b) NP2 and (c) NP3 nanoparticles taken at 40,000× magnification. Scale bar is 2μm.

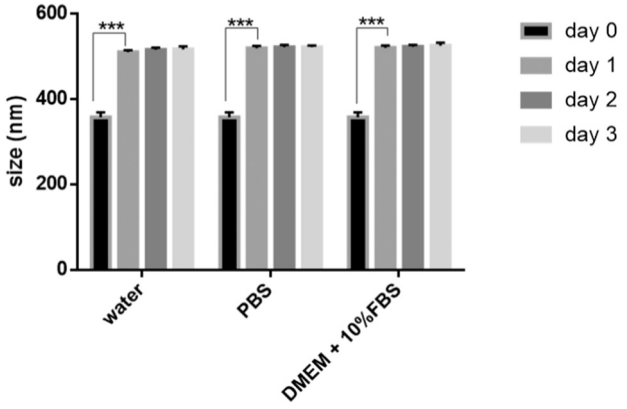

Fig. 3. Structural stability of ChoS (HA/CS) NPs, NP2 formulation was studied in three replicates.

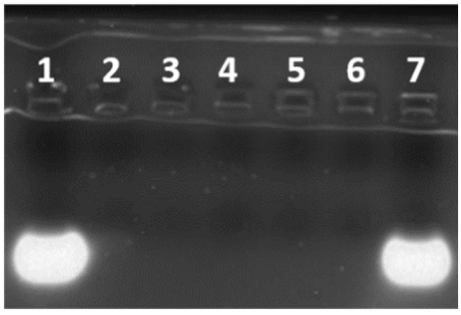

Fig. 4. Gel retardation assay. First lane, control microRNA, second lane, microRNA encapsulated 4.59 μM ChoS (HA/CS) (NP1) NPs, third lane microRNA encapsulated 5.73 μM ChoS (HA/CS) NPs, fourth lane, microRNA encapsulated 6.88 μM ChoS (HA/CS) (NP2), fifth lane, microRNA encapsulated 8.03 μM ChoS (HA/CS), sixth lane, microRNA encapsulated 9.17 μM ChoS (HA/CS) (NP3), seventh lane, microRNA encapsulated 9.17 μM ChoS (HA/CS) NPs incubated with SDS.

free water, 45.14% in PBS and 45.30% in DMEM + 10% FBS medium at the end of the first day ($p \leq 0.001$). The increase in nanoparticle size is due to highly hydrophilic nature of hyaluronic acid and its water retention ability of carboxyl groups forming a loose network [41,43,46]. Besides, neutral pH partially uncharges the chitosan backbone of nanoparticles leading to weak interactions with the anionic groups, resulting a larger size [47]. Stability experiments proved ChoS (HA/CS) NPs are stable nanoparticles and can be used for further applications.

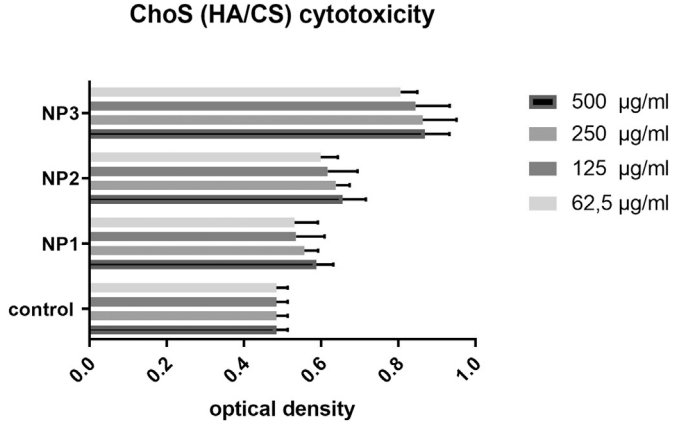

Fig. 6. MTT results of NP1, NP2 and NP3 nanoparticles.

3.3. Gel retardation assay

MicroRNA-149-5p loading to ChoS (HA/CS) NPs were also demonstrated with gel retardation assay. It is seen that naked miRNA migrated into the gel, whereas nanoparticle interaction prevented microRNA to migrate in all nanoparticle formulations. The effect of nanoparticles were also confirmed by SDS treatment, which was incubated with microRNA encapsulated 30:1 N:P ratio ChoS (HA/CS) NPs, prior to gel loading. SDS is known to disrupt electrostatic forces and expected to release microRNAs from nanoparticles in this experiment. The result is seen in the last lane, proving microRNA reappearance after SDS treatment (Fig. 4).

3.4. MicroRNA release from ChoS (HA/CS) NPs

MicroRNA release experiments were performed at 37 °C in PBS under mild stirring. Free microRNA from ChoS (HA/CS) NPs were measured via dialysis and results are shown in Fig. 5. No significant difference was found between the groups in the first 24 h of release experiments. After 24 h, it was observed that NP1 nanoparticles released 8.4%, NP2 nanoparticles 12.2%, NP3 nanoparticles 15.3% of its microRNA content ($p \leq 0.05$). Nanoparticles seem to behave similarly after 48 h and no statistically significant difference was observed between the groups until the end of the release test. At the end of 192 h, 59.03% of the microRNA were released from NP1 nanoparticles, NP2 nanoparticles released 76.27% and NP3 nanoparticles released 76.27% of its microRNA content. This slow release may be the result of strong electrostatic interactions between high molecular weight chitosan and

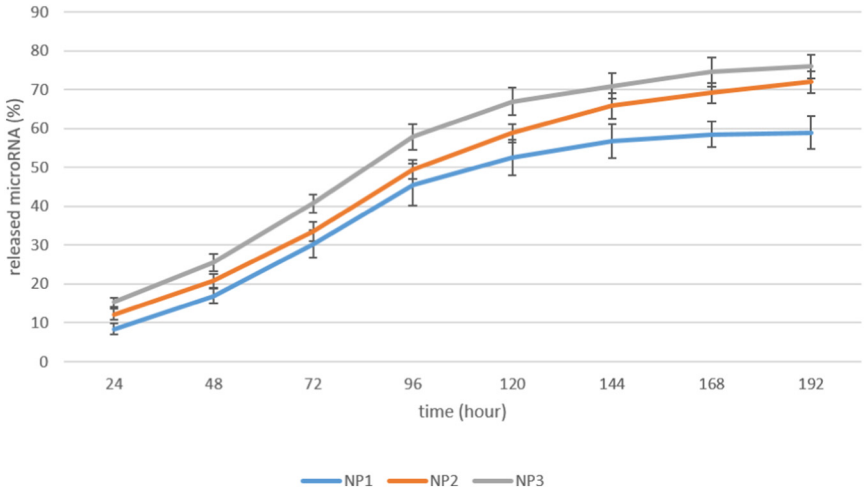

Fig. 5. microRNA release from NP1, NP2 and NP3 nanoparticles in 8 days.

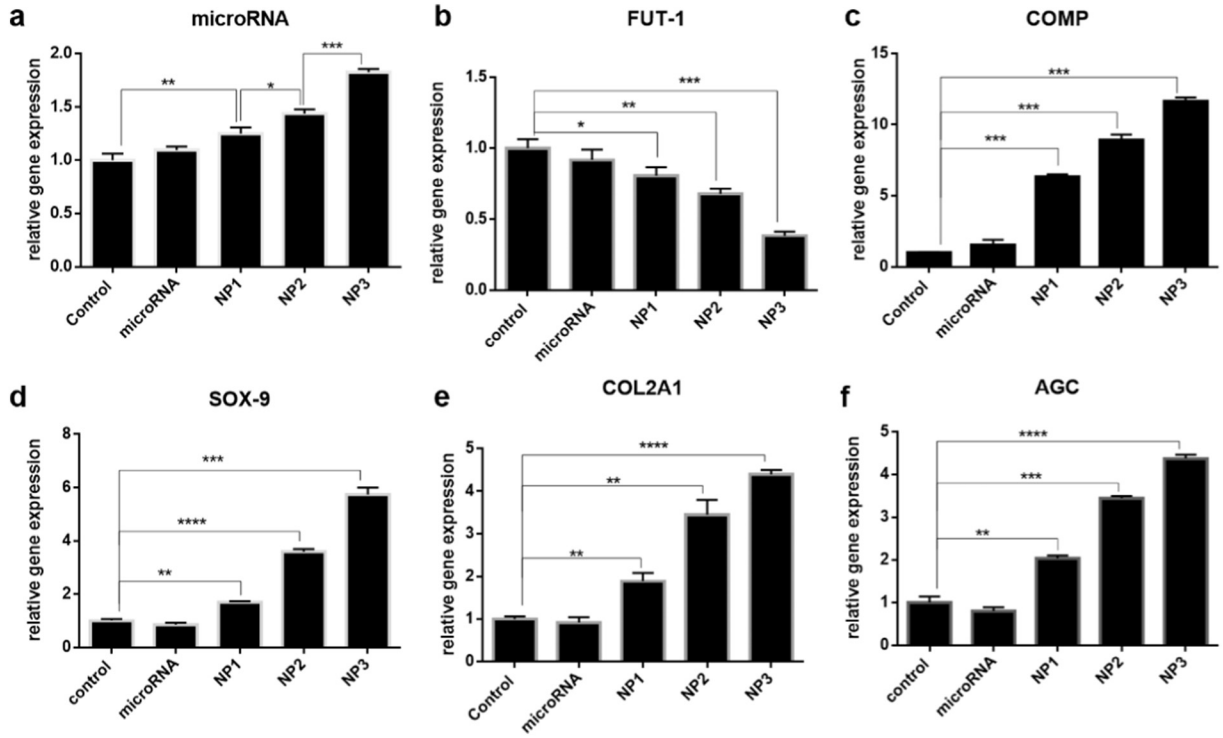

Fig. 7. Gene expression analysis of NP1, NP2 and NP3 (a) microRNA-149-5p, (b) FUT-1, (c) COMP, (d) SOX-9, (e) COL2A1, (f) AGC.

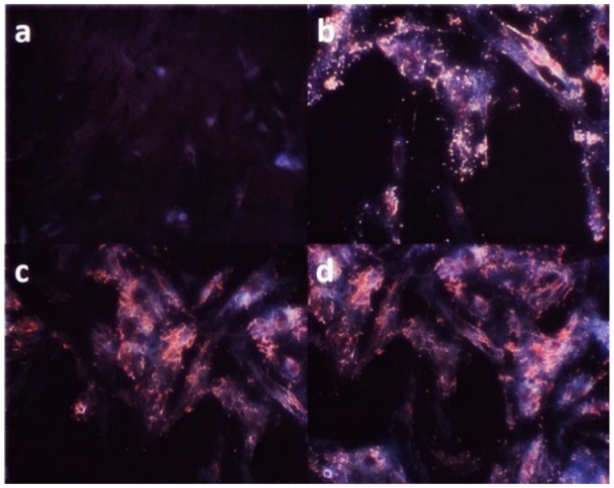

Fig. 8. Safranin O stainings of cells incubated with (a) no particles, (b) NP1, (c) NP2 and (d) NP3 nanoparticles.

chondroitin sulfate. This is also potentially the proof of successful interaction between chondroitin sulfate and HA/CS NPs, as an additional layer of polymer slowed down the microRNA release, which is consistent with the previous reports [48].

3.5. Cytotoxicity of nanoparticles

Fig. 6 shows cell viability of mesenchymal stem cells after incubation with NP1, NP2 and NP3 nanoparticles with different concentrations determined with MTT assay. It is seen that nanoparticles do not show any toxicity until the highest nanoparticle concentration tested. It is seen that increasing chondroitin sulfate amounts lead to an increase in cell viability, due to nature of cells behaving polysaccharides as an energy source, enhancing cell growth [49]. Cytotoxicity experiments showed ChoS (HA/CS) NPs are non-toxic, biocompatible nanoparticles, and can be used for any downstream applications.

3.6. Delivery of microRNA-149-5p in mesenchymal stem cells and gene expression analysis

MicroRNA 149-5p is known to have an important role in cartilage homeostasis, especially in prevention of apoptosis. It has shown that microRNA-149-5p overexpression leads to enhanced chondrocyte proliferation, targeting FUT-1 gene [37]. In this study, microRNA-149-5p encapsulated ChoS (HA/CS) NPs were used for transfection of mesenchymal stem cells, to observe its effects on chondrogenesis and homeostasis. Three different formulations of ChoS (HA/CS) NPs (NP1, NP2 and NP3 nanoparticles) were included in transfection studies, to determine the effects of increasing amounts of chondroitin sulfate. All formulations were set to 100 nM microRNA concentrations. As shown in Fig. 7, successful transfection of microRNA-149-5p was achieved, due to low mRNA levels of target FUT-1 gene and high levels of microRNA-149-5p. The highest microRNA levels were observed in the cells incubated with NP3 nanoparticles, with a 82.98% increase compared to control group ($p < 0.001$). MicroRNA levels increased 43.96% in cells treated with NP2 nanoparticles and 24.88% increase were reported in cells with NP1 nanoparticles (Fig. 7a). The smallest nanoparticles with the highest chondroitin sulfate amount had the highest transfection efficiency, inhibiting the target gene 61,57% ($p \leq 0.001$). Cells incubated with naked microRNA and NP1 did not differ significantly in FUT-1 mRNA levels, NP2 nanoparticles prevent FUT-1 translation 32.04% ($p \leq 0.01$) (Fig. 7b).

Effects of chondroitin sulfate on chondrogenesis were also investigated with gene expression analysis, as they are main components of cartilage ECM. The clear effect of increasing chondroitin sulfate is seen on expression levels of SOX-9 and COMP in Fig. 7c & d, which are the early markers for chondrogenesis [50]. NP3 nanoparticles increased SOX-9 mRNA levels 5-fold and COMP mRNA levels to 10-fold ($p \leq 0.001$). NP2 and NP1 nanoparticles also increased SOX-9 and COMP mRNA levels significantly compared to control group. For chondrocyte markers, AGC and COL2A1 gene expression levels, it was

observed that mRNA levels increase proportionally with increasing chondroitin sulfate amounts (Fig. 7e & f). NP3 and NP2 nanoparticles were shown to increase COL2A1 mRNA levels to 3 fold and 2 fold, respectively. NP1 nanoparticles increased COL2A1 mRNA levels by 88.64% compared to control group ($p \leq 0.01$). For AGC mRNA levels, statistically significant increase ($p \leq 0.01$) were also observed for all experimental groups, proportional with chondroitin sulfate amounts likewise COL2A1 gene expression profiles.

3.7. sGAG staining

Glycosaminoglycan synthesis of mesenchymal stem cells after incubation with ChoS (HA/CS) nanoparticles are represented with Safranin Orange staining (Fig. 8). Images showed glycosaminoglycan synthesis increase with increasing chondroitin sulfate content, highest sGAG staining was observed in cells treated with NP3 nanoparticles. These results are correlated with gene expression analysis, in which SOX-9 and COMP mRNA levels were shown to be increased, as these genes are known to be regulating sGAG synthesis [51,52].

4. Conclusion

To conclude, in this study, microRNA loaded ChoS (HA/CS) nanoparticles were successfully synthesized for simultaneous delivery of a therapeutic gene and cartilaginous matrix components to stem cells, to promote chondrogenesis and downregulate pathological markers regarding osteoarthritis. Chemical and morphological characterizations of nanoparticles were performed before and after microRNA loading. Stability and release behaviour of ChoS (HA/CS) NPs were also determined. Nanoparticles were tested cytotoxically prior to in vitro studies of their transfection efficiencies on mesenchymal stem cells. Results demonstrated a successful transfection of microRNA-149-5p and down-regulation of its target gene, FUT-1. Owing to high polysaccharide content, nanoparticles were also shown to promote synthesis of chondrogenic markers and upregulate responsible genes, which was also demonstrated by cytological staining of sGAG synthesis. Overall, microRNA loaded ChoS (HA/CS) NPs are shown to have a great potential for future applications as combined therapeutic strategies in osteoarthritis treatment.

Acknowledgements

This research did not receive any specific grant from funding agencies in the public, commercial, or not-for-profit sectors.

Appendix A. Supplementary data

Supplementary data to this article can be found online at https://doi.org/10.1016/j.msec.2019.05.006.

References

[1] G. Musumeci, The effect of mechanical loading on articular cartilage, J Funct Morphol Kinesiol (2016) 154–161, https://doi.org/10.3390/jfmk1020154.
[2] A.J. Sophia Fox, A. Bedi, S.A. Rodeo, The basic science of articular cartilage: structure, composition, and function, Sports Health 1 (6) (2009) 461–468, https://doi.org/10.1177/1941738109350438.
[3] D.L. Richter, R.C.S. Jr, D.C. Wascher, Knee articular cartilage repair and restoration techniques: a review, Sports Health 8 (2015) 153–160, https://doi.org/10.1177/1941738115611350.
[4] E.N. Bowman, J.D. Hallock, T.W. Throckmorton, F.M. Azar, Hyaluronic acid injections for osteoarthritis of the knee: predictors of successful treatment, Int. Orthop. (2018) 733–740, https://doi.org/10.1007/s00264-017-3731-8.
[5] D. Zhu, H. Wang, P. Trinh, S.C. Heilshorn, F. Yang, Elastin-like protein-hyaluronic acid (ELP-HA) hydrogels with decoupled mechanical and biochemical cues for cartilage regeneration, Biomaterials 127 (2017) 132–140, https://doi.org/10.1016/j.biomaterials.2017.02.010.
[6] S. Hemmati-sadeghi, J. Ringe, T. Dehne, R. Haag, Hyaluronic acid influence on normal and osteoarthritic tissue-engineered cartilage, Int. J. Mol. Sci. 19 (5) (2018) 15–18, https://doi.org/10.3390/ijms19051519.
[7] M. Neethu, M. Pv, A. Sabareeswaran, N. Prabha, Chitosan-hyaluronic acid hydrogel for cartilage repair, Int. J. Biol. Macromol. 104 (2017) 1936–1945, https://doi.org/10.1016/j.ijbiomac.2017.03.142.
[8] R. Raman, Y. Henrotin, X. Chevalier, A. Migliore, J. Jerosch, J. Montfort, H. Bard, D. Baron, P. Richette, Decision algorithms for the retreatment with viscosupplementation in patients suffering from knee osteoarthritis: recommendations from the EUROpean VIScosupplementation COnsensus group (EUROVISCO), Cartilage (3) (2018) 263–275, https://doi.org/10.1177/1947603517693043.
[9] M. Monet, A. Bozgan, T. Conrozier, Safety and efficacy of single intra-articular injection of a cross-linked hyaluronic acid/mannitol formulation [Happycross®] in knee osteoarthritis results of a prospective observational study in daily practice conditions, OROAJ 5 (2017) 1–5, https://doi.org/10.19080/OROAJ.2017.05.555664.
[10] P.J. Roughley, R.J. White, Age-related changes in the structure of the proteoglycan subunits from human articular cartilage, J. Biol. Chem. (1983) 217–224.
[11] S. Demehri, D. Shakoor, Structural changes in aging-knee vs early-knee osteoarthritis: review of current evidence and future challenges, Osteoarthr. Cartil. 26 (2018) 1412–1414, https://doi.org/10.1016/j.joca.2018.07.005.
[12] P. Pathway, MicroRNA-140 provides robustness to the regulation of hypertrophic chondrocyte differentiation by the, J BMR (2015) 1044–1052, https://doi.org/10.1002/jbmr.2438.
[13] F. Chen, Y. Ni, B. Liu, T. Zhou, C. Yu, Y. Su, X. Zhu, X. Yu, Y. Zhou, Self-crosslinking and injectable hyaluronic acid/RGD-functionalized pectin hydrogel for cartilage tissue engineering, Carbohydr. Polym. 166 (2017) 31–44, https://doi.org/10.1016/j.carbpol.2017.02.059.
[14] X. Zhou, Q. Zhang, L. Chen, W. Nie, W. Wang, H. Wang, X. Mo, C. He, A versatile nanocarrier based on functionalized mesoporous silica nanoparticles to co-deliver osteogenic gene and drug for enhanced osteo-differentiation, ACS Biomater. Sci. Eng. (2019), https://doi.org/10.1021/acsbiomaterials.8b01110 acsbiomaterials.8b01110.
[15] C. Xu, J. Chen, L. Li, X. Pu, X. Chu, X. Wang, M. Li, Y. Lu, X. Zheng, Promotion of chondrogenic differentiation of mesenchymal stem cells by copper: implications for new cartilage repair biomaterials, Mater. Sci. Eng. C 93 (2018) 106–114, https://doi.org/10.1016/j.msec.2018.07.074.
[16] A.R. Armiento, M.J. Stoddart, M. Alini, D. Eglin, Biomaterials for articular cartilage tissue engineering: learning from biology, Acta Biomater. 65 (2018) 1–20, https://doi.org/10.1016/j.actbio.2017.11.021.
[17] Y. Liu, G. Zhou, Y. Cao, Recent progress in cartilage tissue engineering — our experience and future directions, Engineering 3 (2017) 28–35, https://doi.org/10.1016/J.ENG.2017.01.010.
[18] G. Wu, C. Feng, G. Hui, Z. Wang, J. Tan, L. Luo, P. Xue, Q. Wang, X. Chen, Improving the osteogenesis of rat mesenchymal stem cells by chitosan-based-microRNA nanoparticles, Carbohydr. Polym. 138 (2016) 49–58, https://doi.org/10.1016/j.carbpol.2015.11.044.
[19] L. Zhao, M. Liu, J. Wang, G. Zhai, Chondroitin sulfate-based nanocarriers for drug/gene delivery, Carbohydr. Polym. 133 (2015) 391–399, https://doi.org/10.1016/j.carbpol.2015.07.063.
[20] T. Tenkumo, J.R. Vanegas Sáenz, K. Nakamura, Y. Shimizu, V. Sokolova, M. Epple, Y. Kamano, H. Egusa, T. Sugaya, K. Sasaki, Prolonged release of bone morphogenetic protein-2 in vivo by gene transfection with DNA-functionalized calcium phosphate nanoparticle-loaded collagen scaffolds, Mater. Sci. Eng. C 92 (2018) 172–183, https://doi.org/10.1016/j.msec.2018.06.047.
[21] Y. Pi, X. Zhang, Z. Shao, F. Zhao, X. Hu, Y. Ao, Intra-articular delivery of anti-Hif-2 α siRNA by chondrocyte-homing nanoparticles to prevent cartilage degeneration in arthritic mice, Gene Ther. (2015) 439–448, https://doi.org/10.1038/gt.2015.16.
[22] S. Yeon, J. Sun, H. Na, H. Jin, S. Won, H. Park, K. Park, Co-delivery of Cbfa-1-targeting siRNA and SOX9 protein using PLGA nanoparticles to induce chondrogenesis of human mesenchymal stem cells, Biomaterials 35 (2014) 8236–8248, https://doi.org/10.1016/j.biomaterials.2014.05.092.
[23] H.D. Lu, H. Zhao, K. Wang, L. Lv, Novel hyaluronic acid chitosan nanoparticles as non-viral gene delivery vectors targeting osteoarthritis, IJP 420 (2011) 358–365.
[24] J.T. Oliveira, R.L. Reis, Polysaccharide-based materials for cartilage tissue engineering applications, J. Tissue Eng. Regen. Med. (2011) 421–436, https://doi.org/10.1002/term.
[25] L. Bian, D.Y. Zhai, E. Tous, R. Rai, R.L. Mauck, J.A. Burdick, Enhanced MSC chondrogenesis following delivery of TGF-b3 from alginate microspheres within hyaluronic acid hydrogels in vitro and in vivo, Biomaterials 32 (2011) 6425–6434, https://doi.org/10.1016/j.biomaterials.2011.05.033.
[26] D. Yoon, H. Park, S. Woo, J. Won, K. Yong, Injectable hydrogels prepared from partially oxidized hyaluronate and glycol chitosan for chondrocyte encapsulation, Carbohydr. Polym. 157 (2017) 1281–1287, https://doi.org/10.1016/j.carbpol.2016.11.002.
[27] C. Qi, J. Liu, Y. Jin, L. Xu, G. Wang, Z. Wang, L. Wang, Photo-crosslinkable, injectable sericin hydrogel as 3D biomimetic extracellular matrix for minimally invasive repairing cartilage, Biomaterials 163 (2018) 89–104, https://doi.org/10.1016/j.biomaterials.2018.02.016.
[28] T.A. Debele, S.L. Mekuria, H. Tsai, Polysaccharide based nanogels in the drug delivery system: application as the carrier of pharmaceutical agents, Mater. Sci. Eng. C 68 (2016) 964–981, https://doi.org/10.1016/j.msec.2016.05.121.
[29] T. Nochi, Y. Yuki, H. Takahashi, S. Sawada, M. Mejima, T. Kohda, N. Harada, I.G. Kong, A. Sato, N. Kataoka, D. Tokuhara, S. Kurokawa, Y. Takahashi, H. Tsukada, S. Kozaki, K. Akiyoshi, Nanogel antigenic protein-delivery system for adjuvant-free intranasal vaccines, Nat. Mater. 9 (2010) 572–578, https://doi.org/10.1038/nmat2784.
[30] H. Li, X. Yang, F. Gao, C. Qian, C. Li, Bioreduction-ruptured nanogel for switch on/off release of Bcl2 siRNA in breast tumor therapy, J. Control. Release (2018) 78–90,

https://doi.org/10.1016/j.jconrel.2018.02.036.
[31] Y.P. Li, X.C. Wei, P.C. Li, C.W. Chen, X.H. Wang, Q. Jiao, D.M. Wang, F.Y. Wei, J.Z. Zhang, L. Wei, The role of miRNAs in cartilage homeostasis, Curr Genomics (2015) 393–404, https://doi.org/10.2174/1389202916666150817203144.
[32] T. Kim, J.U. Kim, K. Yang, K. Nam, D. Choe, E. Kim, I.-H. Hong, M. Song, H. Lee, J. Park, Y.H. Roh, Nanoparticle-patterned multicompartmental chitosan capsules for oral delivery of oligonucleotides, ACS Biomater. Sci. Eng. 4 (2018) 4163–4173, https://doi.org/10.1021/acsbiomaterials.8b00806.
[33] M. Nugent, MicroRNAs: exploring new horizons in osteoarthritis, Osteoarthr. Cartil. 24 (2016) 573–580, https://doi.org/10.1016/j.joca.2015.10.018.
[34] L. Cong, Y. Zhu, G. Tu, A bioinformatic analysis of microRNAs role in osteoarthritis, Osteoarthr. Cartil. 25 (2017) 1362–1371, https://doi.org/10.1016/j.joca.2017.03.012.
[35] J. Peng, S. Chen, C. Wu, H. Chong, Y. Ding, A. Shiau, C. Wang, Amelioration of experimental autoimmune arthritis through targeting of synovial fibroblasts by intraarticular delivery of microRNAs 140-3p and 140-5p, Arthritis Rheum. 68 (2016) 370–381, https://doi.org/10.1002/art.39446.
[36] R.M. Raftery, D.P. Walsh, I.M. Castaño, A. Heise, G.P. Duffy, S. Cryan, F.J.O. Brien, Delivering nucleic-acid based nanomedicines on biomaterial scaffolds for orthopedic tissue repair: challenges, progress and future perspectives, Adv. Mater. (2016) 5447–5469, https://doi.org/10.1002/adma.201505088.
[37] Z. Wang, J. Hu, Y. Pan, Y. Shan, L. Jiang, X. Qi, L. Jia, miR-140-5p/miR-149 affects chondrocyte proliferation, apoptosis, and autophagy by targeting FUT1 in osteoarthritis, Inflammation (2018), https://doi.org/10.1007/s10753-018-0750-6.
[38] X. Deng, M. Cao, J. Zhang, K. Hu, Z. Yin, Z. Zhou, X. Xiao, Y. Yang, W. Sheng, Y. Wu, Y. Zeng, Hyaluronic acid-chitosan nanoparticles for co-delivery of MiR-34a and doxorubicin in therapy against triple negative breast cancer, Biomaterials 35 (2014) 4333–4344, https://doi.org/10.1016/j.biomaterials.2014.02.006.
[39] M. De Fuente, B. Seijo, M.J. Alonso, Novel hyaluronic acid-chitosan nanoparticles for ocular gene therapy, IOVS 49 (2018) 2016–2024, https://doi.org/10.1167/iovs.07-1077.
[40] T.V. Nguyen, T. Thu, H. Nguyen, S. Wang, T. Phuong, K. Vo, A.D. Nguyen, Preparation of chitosan nanoparticles by TPP ionic gelation combined with spray drying, and the and a chitosan nanoparticle – amoxicillin complex, Res. Chem. Intermed. 43 (2017) 3527–3537, https://doi.org/10.1007/s11164-016-2428-8.
[41] S. Al-qadi, M. Alatorre-meda, M. Martin-pastor, P. Taboada, C. Remu, The role of hyaluronic acid inclusion on the energetics of encapsulation and release of a protein molecule from chitosan-based nanoparticles, Colloids Surf. B. 141 (2016) 223–232, https://doi.org/10.1016/j.colsurfb.2016.01.029.
[42] G. Pitarresi, E.F. Craparo, F.S. Palumbo, B. Carlisi, G. Giammona, T. Farmaceutiche, Composite nanoparticles based on hyaluronic acid chemically cross-linked with r, -polyaspartylhydrazide, Biomacromolecules (2007) 1890–1898, https://doi.org/10.1021/bm070224a.
[43] J. Berger, M. Reist, J.M. Mayer, O. Felt, N.A. Peppas, R. Gurny, Structure and interactions in covalently and ionically crosslinked chitosan hydrogels for biomedical applications, EJPB 57 (2004) 19–34, https://doi.org/10.1016/S0939-6411(03)00161-9.
[44] H. Wang, S. Liu, L. Jia, F. Chu, Y. Zhou, Z. He, M. Guo, C. Chen, L. Xu, Nanostructured lipid carriers for MicroRNA delivery in tumor gene therapy, Cancer Cell Int. (2018) 1–6, https://doi.org/10.1186/s12935-018-0596-x.
[45] L. Zhang, X. Yang, Y. Lv, X. Xin, C. Qin, X. Han, L. Yang, Cytosolic co-delivery of miRNA-34a and docetaxel with core-shell nanocarriers via caveolae-mediated pathway for the treatment of metastatic breast cancer, Nat. Publ. Gr. (2017) 1–16, https://doi.org/10.1038/srep46186.
[46] S. Al-qadi, M. Alatorre-meda, E.M. Zaghloul, P. Taboada, C. Remunán-lópez, Chitosan – hyaluronic acid nanoparticles for gene silencing: the role of hyaluronic acid on the nanoparticles' formation and activity, Colloids Surf. B. 103 (2013) 615–623, https://doi.org/10.1016/j.colsurfb.2012.11.009.
[47] T. Rojanarata, P. Opanasopit, S. Techaarpornkul, T. Ngawhirunpat, Chitosan-thiamine pyrophosphate as a novel carrier for siRNA delivery, Pharm. Res. 25 (2008) 0–7, https://doi.org/10.1007/s11095-008-9648-6.
[48] I. Fernandez-piñeiro, A. Pensado, I. Badiola, A. Sanchez, Development and characterisation of chondroitin sulfate- and hyaluronic acid-incorporated sorbitan ester nanoparticles as gene delivery systems, Eur. J. Pharm. Biopharm. 125 (2018) 85–94, https://doi.org/10.1016/j.ejpb.2018.01.009.
[49] D. Sow, Z. Leong, J. Gek, L. Tan, C.L. Chin, S.Y. Mak, Y.S. Ho, Evaluation and use of disaccharides as energy source in protein-free mammalian cell cultures, Nat. Publ. Gr. (2017) 1–10, https://doi.org/10.1038/srep45216.
[50] F. Barry, R.E. Boynton, B. Liu, J.M. Murphy, B.E.T. Al, Chondrogenic differentiation of mesenchymal stem cells from bone marrow: differentiation-dependent gene expression of matrix components, Exp. Cell Res. 200 (2001) 189–200, https://doi.org/10.1006/excr.2001.5278.
[51] S.P. Henry, S. Liang, K.C. Akdemir, B. Crohmbrugge, The postnatal role of Sox9 in cartilage, J. Bone Miner. Res. 27 (2013) 2511–2525, https://doi.org/10.1002/jbmr.1696.
[52] H. Haleem-smith, R. Calderon, Y. Song, R.S. Tuan, H. Faye, Cartilage oligomeric matrix protein enhances, Cartilage 113 (2013) 1245–1252, https://doi.org/10.1002/jcb.23455.CARTILAGE.